Oxygen Toxicity and Iron Accumulation in the Lungs of Mice Lacking Heme Oxygenase-2

Phyllis A. Dennery,* Douglas R. Spitz,‡ Guang Yang,* Arthur Tatarov,* Christen S. Lee,* Mychelle L. Shegog,* and Kenneth D. Poss§

**Department of Pediatrics, Stanford University School of Medicine, Stanford, California 94305; ‡Cancer Biology, Radiation Oncology Center, Washington University School of Medicine, St. Louis, Missouri 63110; and §Howard Hughes Medical Institute, Department of Biology, Massachusetts Institute of Technology, Cambridge, Massachusetts 02139*

Abstract

Heme oxygenase (HO) activity leads to accumulation of the antioxidant bilirubin, and degradation of the prooxidant heme. Moderate overexpression of the inducible form, HO-1, is associated with protection against oxidative injury. However, the role of HO-2 in oxidative stress has not been explored. We evaluated survival, indices of oxidative injury, and lung and HO expression in HO-2 null mutant mice exposed to $> 95\%$ O_2 compared with wild-type controls. Similar basal levels of major lung antioxidants were observed, except that the knockouts had a twofold increase in total glutathione content. Despite increased HO-1 expression from HO-1 induction, knockout animals were sensitized to hyperoxia-induced oxidative injury and mortality, and also had significantly increased markers of oxidative injury before hyperoxic exposure. Furthermore, during hyperoxia, lung hemoproteins and iron content were significantly increased without increased ferritin, suggesting accumulation of available redox-active iron. These results demonstrate that the absence of HO-2 is associated with induction of HO-1 and increased oxygen toxicity in vivo, apparently due to accumulation of lung iron. These results suggest that HO-2 functions to augment the turnover of lung iron during oxidative stress, and that this function does not appear to be compensated for by induction of HO-1 in the knockouts. (*J. Clin. Invest.* 1998. 101:1001–1011.) Key words: hyperoxia • iron • ferritin • glutathione • knockout

Introduction

Heme oxygenase (HO)[1] is known to catalyze degradation of heme and formation of bilirubin and carbon monoxide (CO). The inducible form, HO-1, is a known stress protein that is regulated by a wide variety of oxidative stresses (1–4) including hyperoxia (5–7). In fact, induction of this enzyme is felt to be a generalized response to oxidative stress manifested by glutathione depletion and oxidative degradation of protein (8–10). Furthermore, the distal enhancer of the HO-1 gene contains several AP-1 binding sites that show regulation in oxidative stress (11). Since HO-1 is readily inducible in oxidant stress, and the reactions of HO lead to degradation of a prooxidant (heme) and to formation of an antioxidant (bilirubin), a cytoprotective role is theorized for HO. Another way in which increased HO activity may protect against hyperoxia is through coinduction of ferritin due to iron release from heme. In a variety of in vitro transfection models, HO-1 has been shown by us and others to play a role in protection against oxidative stress (2, 5, 13, 14). Whereas in all of these examples, manipulation of HO-1 in vitro was associated with altering cellular antioxidant status, no reports have documented the effects of manipulation of HO-2, the constitutive isoform of HO. Since both HO-1 and HO-2 catalyze the same reaction, albeit at differing kinetic rates, both should possess similar antioxidant functions if the antioxidant benefit results solely from the reaction byproducts of HO. However, in a recent publication, HO-2 has been shown to serve as a heme-binding protein since it has two heme-binding sites not involved in heme catalysis (15). This result may suggest that HO-2, unlike HO-1, serves to sequester heme, thereby possibly decreasing the availability of heme for participation in oxidative reactions. Nonetheless, the role of HO-2 in antioxidant defense has not been studied, and it is not known whether HO-1 induction serves in protection against oxidative stress in vivo.

To better understand the mechanism by which HO-2 affects lung antioxidant defense, we used a previously characterized null mutant mouse model lacking HO-2 (henceforth referred to as HO-2 knockouts), and examined survival in chronic hyperoxia (> 7 d) as well as parameters of oxidative injury and HO expression in lung homogenates and frozen lung sections as compared with wild-type controls after sublethal (3 d) hyperoxic exposure. The perceived advantages of this model over pharmacologic alteration of HO activity is that specific inhibition of HO-2–related activity is possible, whereas with pharmacologic agents, differentiation of HO-1 vs. HO-2 activities would not be possible. In further attempts to understand the mechanism by which HO-2 may mediate its biological effects, we evaluated heme and iron content in the lungs of the transgenic animals since accumulation of heme and heme iron could potentially exacerbate prooxidant effects.

Methods

Animal model

Homozygote HO-2 null mutants were obtained by targeted disruption of the HO-2 gene as previously described (16). These animals

Address correspondence to Phyllis A. Dennery, M.D., Department of Pediatrics, Stanford University School of Medicine, 750 Welch Rd. #315, Palo Alto, CA 94304. Phone: 650-723-5711; FAX: 650-725-8351; E-mail: mn.phd@forsythe.stanford.edu

Received for publication 21 April 1997 and accepted in revised form 18 December 1997.

1. *Abbreviations used in this paper:* CO, carbon monoxide; HO, heme oxygenase; LPO, lipid hydroperoxidases; NO, nitric oxide; TBA-RS, thiobarbituric acid–reactive substances.

J. Clin. Invest.

0021-9738/98/03/1001/11 $2.00
Volume 101, Number 5, March 1998, 1001–1011
http://www.jci.org

were shown to have absence of HO-2 mRNA and decreased HO activity in the brain and other tissues. Nonetheless, the animals were morphologically indistinct from their wild-type counterparts, and were fertile (16). Animal protocols were reviewed and approved by the Animal Care Institutional Review Panel of Stanford University.

Experimental design

2-mo-old HO-2 +/+ or HO-2 −/− B6/129 mice were kept in a 12-h light/dark cycle and given water and food ad libitum. After 2–3 d of recovery from transport, the animals were placed in an airtight Plexiglass cylindrical exposure chamber (Vreman Scientifics, Los Altos, CA) that had a port for gas entry and access to food and water. Greater than 95% oxygen (hyperoxia) was provided with commercial cylinders (Liquid Carbonic, Chicago, IL) in a flow-through system. After 3 d of exposure, the animals were killed by CO_2 narcosis. Blood was obtained by percutaneous intracardiac puncture with a 21 G needle, and serum was separated by centrifugation. The lungs were excised and rinsed in cold PBS on ice to remove any blood.

A subgroup of animals were also exposed chronically to hyperoxia (> 7 d), using the same protocol outlined above. The number of surviving animals were determined daily for each group until all animals had died. Average survival was then determined for both groups (wild-types and knockouts).

In other experiments, animals were injected intraperitoneally with 15 mg/kg hemin (Sigma Chemical Co., St. Louis, MO), a known inducer of ferritin, to evaluate whether differences in heme-mediated ferritin induction could be observed between the wild-type and knockout animals. 24 h later, the lungs were excised and homogenized for further analysis.

Preparation of histological sections

After careful rinsing with cold isotonic saline, whole lungs were excised along with the trachea, inflated with embedding medium (O.C.T. compound; Miles Inc., Elkhart, IN) to distend the airways, allowed to freeze on dry ice, and then stored at −80°C. The frozen samples were later cut onto positively charged slides to a 6-μm thickness using a Reickert-Young cryostat (Cambridge Instruments, Buffalo, NY). Tissue morphology was verified by hematoxylin and eosin staining.

Determination of oxidative injury

Susceptibility to lipid peroxidation (thiobarbituric acid–reactive substances; TBA-RS) was assessed in lung homogenates incubated with 0.1 M phosphate buffer containing 50 μm ADP and 1 mM $FeCl_3$ for 1 h at 37°C. Thereafter, 0.3 ml 10% trichloroacetic acid and 0.6 ml 0.5% thiobarbituric acid solution were added, and samples were boiled for 15 min. The samples were centrifuged at 5,000 *g,* absorbance was read at 535 nm, and values were determined using an extinction coefficient of $1.55 \times 10\ M^{-1}\ cm^{-1}$.

Serum lipid hydroperoxides (LPO) were measured in animals using a commercially available kit that allows for detection of hydroperoxides without interfering substances (LPO Determiner Kit; Kamiya Chemicals, Kyoto, Japan).

Lung protein oxidation was estimated using Western analysis of the protein carbonyl content by a modification of the method of Shacter et al. (18) as previously described (13). To compare the extent of protein oxidation, densitometric quantitation of the same band consistently showing the strongest signal in all samples was performed.

To ensure that the transgenic animals did not differ in levels of other antioxidants, and only had differences in HO, a variety of lung antioxidants was measured before exposure. Lung tissue was homogenized in cold 50 mM phosphate buffer containing 1.34 mM diethylenetriaminepentaacetic acid. An aliquot of each sample was assayed for protein content (19). Aliquots of samples were then mixed with 5% sulfosalicylic acid to obtain a diluted sample for determination of total glutathione content using the method of Anderson (20), and were expressed as μg total GSH/mg protein. Gamma-glutamyl transferase activity was detected using a commercially available kit (No. 419; Sigma Chemical Co.). Glutathione peroxidase activity was assayed by the method of Lawrence and Burk (21) using cumene hydroperoxide as substrate. Catalase activity was determined by the method of Beers and Sizer (22), and was expressed as kU/mg protein as described by Aebi (23). Total superoxide dismutase activity was determined by the method of Spitz and Oberley (24) and expressed as U/mg protein. Serum vitamin E was determined by a commercial laboratory (University of Michigan Laboratories, East Lansing MI).

Determination of HO activity

Tissues were analyzed for HO activity by gas chromatography as previously described (25), in subdued lighting. Homogenates were analyzed for protein content by the method of Lowry et al. (19), and read at absorbance 595 nm. HO activity was expressed as nmol CO/mg protein/h.

Antibodies

Polyclonal rabbit anti–rat HO-1 antibodies were raised against a 30-kD soluble HO-1 protein expressed in *Escherichia coli* from rat liver cDNA (26; gift of Angela Wilks, University of California San Francisco, CA) as previously described (5). Rabbit anti–rat HO-2 antibodies were obtained from Stressgen Biotechnologies Corp., (Victoria, B.C., Canada).

Determination of HO-1 and HO-2 immunoreactive protein levels (Western analysis)

For detection of HO-1 and HO-2 immunoreactive protein, 20-μg aliquots of lung homogenates were electrophoresed on a 12% polyacrylamide gel and incubated overnight with a 1:600 dilution of rabbit anti–rat HO-1 IgG (5). Antigen–antibody complexes were visualized with the horseradish peroxidase chemiluminesence system according to the manufacturer's instructions (Bio-Rad Laboratories, Richmond, CA). Blots were subsequently washed in Tris-buffered saline with 0.1% Tween overnight and reincubated for 2 h with a 1:800 dilution of rabbit anti–rat HO-2 IgG, and antigen antibody complexes were visualized as described above. Equal loading was verified by Coomassie blue staining. Quantification was performed by densitometry (PDI, Sunnyvale, CA).

Immunohistochemical localization of HO-1

Immunohistochemical staining of HO-1 protein was accomplished with 6-μm frozen tissue sections. The slides were fixed in ice-cold 100% acetone. The tissues were permeabilized in 0.3% saponin in PBS and blocked in a PBS solution containing 5% nonfat powdered milk, 1% BSA, and 0.03% saponin. The slides were then incubated with a 1:25 dilution of rabbit anti–rat HO-1 antibodies overnight in a humidified chamber. After incubation, the slides were washed twice in PBS containing 0.03% saponin and 1% milk, and were further incubated with a 1:50 dilution of Texas red–conjugated goat anti–rabbit antibodies (Southern Biotechnologies, Inc., Birmingham, AL) for 2 h at 37°C. To see whether the HO-1 signal colocalized to alveolar macrophages, the slides were washed and finally incubated for 3 h at 37°C with monoclonal FITC-labeled rat anti–mouse macrophage monoclonal antibodies (Biosource International, Camarillo, CA) at a 1:10 dilution. The slides were then mounted with antifade reagent in glycerol buffer (Slowfade; Molecular Probes, Inc., Eugene, OR) and viewed with a fluorescence microscope/confocal laser scanning unit (Model 2010; Molecular Dynamics, Inc., Sunnyvale, CA). Excitation was set at 488 nm, and emission at 515–545 nm for FITC. For Texas red, excitation was set at 568 nm and emission at > 590 nm. Images were processed as anaglyphs on a SGI computer system (Molecular Dynamics, Inc.). Negative controls for nonspecific binding incubated with secondary antibody only, were processed and revealed no signal.

Determination of HO-1 and HO-2 mRNA levels

Plasmid and probe preparation. The plasmid pBKRHO1 was constructed in pBluescript II SK- using a rat HO-1 cDNA fragment pre-

pared by RT-PCR as previously described (5). The housekeeping genes β-actin (American Type Culture Collection, Rockville, MD) and GAPD were prepared as an Eco RI digest of the HHCPF19 plasmid by standard methods (27). Labeled probes were prepared by the random primer method (28) using [^{32}P]dCTP.

Northern hybridization. RNA was isolated by the guanidinium thiocyanate/phenol extraction method (29) and quantitated spectrophotometrically at 260 nm. RNA (20 μg) was electrophoresed and probed as previously described (5). For reprobing, membranes were stripped according to the manufacturer's protocol using boiling 0.5% SDS. HO-1, HO-2, and β-actin mRNA quantification was performed by densitometry, and the ratio of HO-1 to β-actin and/or GAPD was calculated.

Determination of lung heme, iron, transferrin and ferritin content

For determination of lung heme content, microsomes were prepared as previously described (30). These were washed twice with cold 0.15 M KCl and centrifuged to recover the microsomal pellet. The samples were then resuspended in 0.9% NaCl, mixed with a solution of 25% (vol/vol) pyridine in 0.075 M NaOH, and scanned at an absorbance of 350–600 nm. The absorbance peak corresponding to the heme Sorret band (414 nm) was quantitated using a molar extinction coefficient of $\beta \times 10^{-6}/2.303 = \epsilon_{mM}$ as published (31). Values were expressed as mM heme/mg protein.

Hemoprotein content of lung tissues was determined using a modification of the method of Bonfils et al. (32) as previously described (13). The gel was then briefly washed in PBS and visualized using an intensified CCD camera (Hamamatsu Photonics, Bridgewater, NJ). The camera was fitted with a 60-mm macrolens, and images were processed using an Aegus 50 image processor (Hamamatsu Photonics) and archived on a 486 IBM workstation. Grayscale images representing photon emission were obtained by integrating over 15 min. The images were transferred to a Macintosh Power PC and superimposed using Adobe Photoshop Software. Images were displayed at a bit range of 0–3.

To assess total lung iron (heme, nonheme, and low relative molecular mass iron), samples were treated with 0.2% (vol/vol) nitric acid overnight and then subjected to graphite furnace atomic absorption spectrometry using a Perkin Elmer 2380 atomic absorption spectrometer and a HGA-700 graphite furnace. The furnace temperature was gradually ramped to a preatomization temperature of 750°C and then directly elevated to the atomization temperature of 2700°C with measurement at 248.3 nm (33).

To assess iron available to stimulate free radical reactions (reactive iron), samples were reacted with bleomycin in the presence of DNA and ascorbic acid as previously described (34). This assay allows for detection of iron ions bound to low molecular mass agents or loosely bound to proteins, but does not allow for detection of iron bound to hemoproteins (35).

To assess iron deposition in the lung, 6-μm frozen lung sections from transgenic and wild-type animals were fixed in 0.5% glutaraldehyde in PBS for 10 min. After rinsing in PBS, the slides were incubated with Perl's solution (1:1, 2% HCl and 2% potassium ferricyanide) at room temperature for 30 min. Sections were then rinsed in PBS and incubated in diaminobenzidine (DAB) and urea-H_2O (Sigma Chemical Co.) in deionized water for 20 min. The reaction was stopped by rinsing in PBS. Lung sections were counterstained with Gill no. 3 hematoxylin (Sigma Chemical Co.; 36).

Ferritin protein levels were estimated in the lung homogenates using Western analysis. The samples were electrophoresed on a 12% polyacrylamide gel which was then transferred onto PVDF membrane as described above (see Western analysis for HO-1 and HO-2 section). The membranes were incubated with a 1:1,000 dilution of rabbit anti–rat ferritin antibodies (gift of R.S. Eisenstein, University of Wisconsin, Madison, WI) and then complexed with a 1:5,000 dilution of HRP-labeled goat anti–rabbit IgG and visualized by chemiluminescence (ECL kit; Amersham Corp., Arlington Heights, IL). Densitometric quantitation of the bands corresponding to ferritin was performed. Equal loading of the samples was verified with Coomassie blue staining. To compare the level of ferritin protein, densitometric quantitation of the bands corresponding to the ferritin heavy and light chains were performed.

Tissue iron content is determined by iron influx through transferrin or decreased iron reuse (37). As an index of transferrin activity, transferrin receptor immunoreactive protein was determined by incubating lung slices with a 1:25 dilution of rat anti–mouse transferrin receptor IgG antibody (gift of Dr. John D. Kemp, University of Iowa, Iowa City, IA) for 3 h at 37°C followed by incubation with a 1:50 dilution of FITC-labeled mouse anti–rat IgG (Jackson ImmunoResearch Labs, Inc., West Grove, PA). Immunofluorescent signal was visualized by confocal microscopy as described above.

Ferritin expression can be modified by factors including nitric oxide (NO; 38). To assess whether changes in NO production could account for the changes observed in ferritin content, lung homogenates were evaluated for nitrotyrosine residues by Western analysis. Nitrotyrosine residues have been previously shown to be markers for proteins interacting with NO in vivo (39). In brief, lung homogenates were electrophoresed on a 12% SDS polyacrylamide gel along with nitrotyrosine molecular weight standards. The gel was then transferred onto a nitrocellulose membrane. The membrane was washed in water and blocked in 1% gelatin for 20 min at room temperature. Rabbit polyclonal anti–nitrotyrosine antibodies (Upstate Biotechnology Inc., Lake Placid, NY) were diluted 1:1,000 in fresh PBS with 3% nonfat dry milk and used for incubation overnight at 4°C. After two washes in water, the membrane was incubated with a goat anti–rabbit IgG linked to horseradish peroxidase at a 1:3,000 dilution for 1.5 h at room temperature. The membrane was finally washed once in PBS with 0.05% Tween and rinsed four times in water. Immune complexes were visualized by chemiluminescence (ECL kit; Amersham Corp.). To compare the extent of nitration, densitometric quantitation of all the bands visualized was performed in each sample.

Statistical analysis

For comparison between transgenic and wild-type mice in air or hyperoxia, the Null hypothesis that there was no difference between

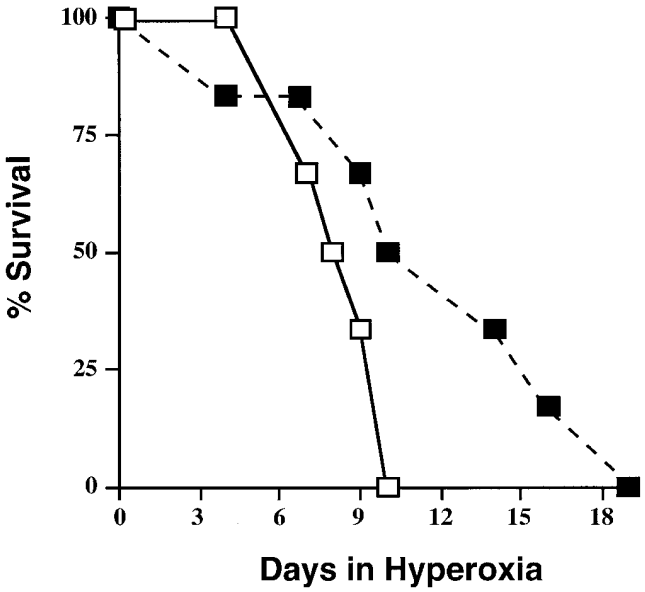

Figure 1. Survival of HO-2 knockout and wild-type mice in hyperoxia. Six animals from each group were exposed to > 95% O_2 for > 7 d until all animals had died. The number of surviving animals were plotted for each day. □, knockout; ■, wild-type.

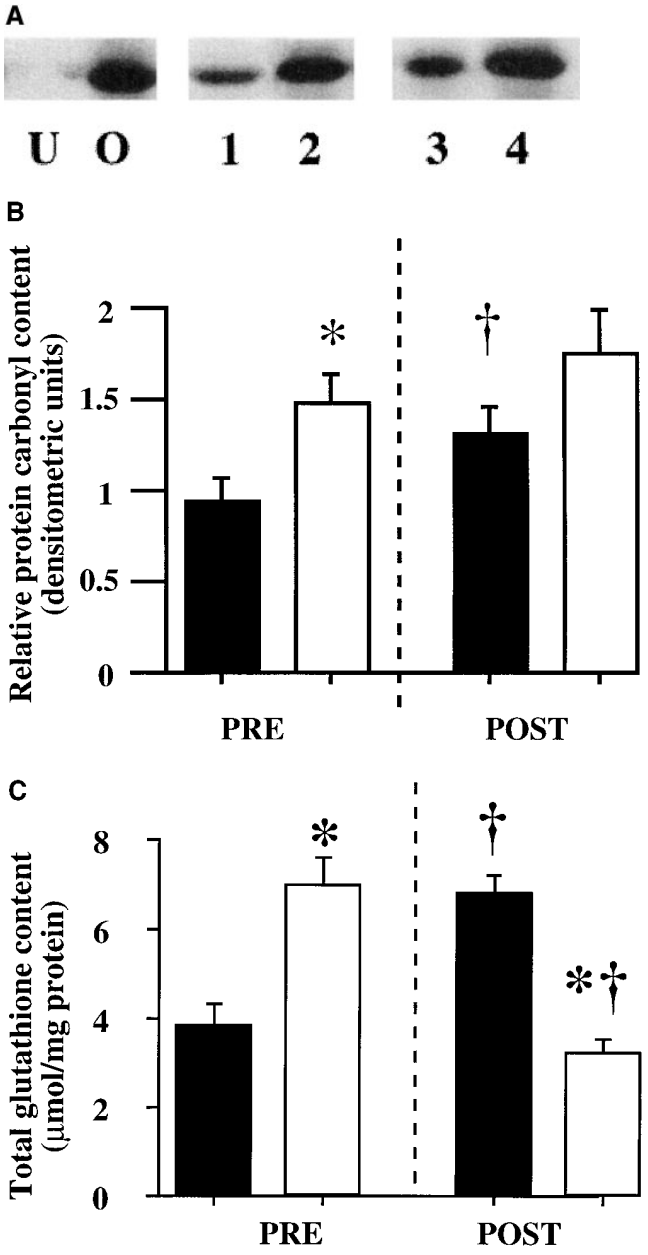

Figure 2. (*A*) Detection of protein carbonyl in the lungs of HO-2 knockout and wild-type mice before and after hyperoxic exposure by Western analysis for anti-DNP antibodies (see Methods). Representative example of four analyses. Controls were as follows: *U* (negative control), unoxidized protein molecular weight standard mixture treated with DNPH as described; *O* (positive control), protein molecular weight standard mixture oxidized overnight with 100 μM ferric chloride and 25 mM ascorbic acid to induce oxidation, and then subjected to DNPH incubation as described. Lane *1*, wild-type, preexposure; lane *2*, knockout, preexposure; lane *3*, wild-type, posthyperoxic exposure; lane *4*, knockout, posthyperoxia. (*B*) Relative protein carbonyl content of the lungs of HO-2 knockout and wild-type mice before and after hyperoxic exposure. Values were determined by densitometric evaluation of the bands detected in the samples represented in Fig. 2 *A*. Densitometric values for each sample were then normalized to the values for the wild-type before exposure value in each membrane to allow for comparison between membranes. Each *bar* represents the mean±SE of five lungs from different animals. Knockouts are represented by the *open bars* and wild-types by the *solid bars*. *$P < 0.05$ vs. wild-type; †$P < 0.05$ vs. the same group before exposure. (*C*) Total glutathione content of the lungs of HO-2 knockout and wild-type mice before and after hyperoxic exposure. Each *bar* represents the mean±SE of five lungs from different animals. Knockouts are represented by the *open bars*, and wild-types by the *solid bars*. *$P < 0.05$ vs. wild-type; †$P < 0.05$ vs. same group, preexposure.

Table I. Lung Antioxidant Levels in Wild-type and HO-2 Knockout Mice Before Hyperoxic Exposure

Antioxidant	WT	KO	*P* value
Total glutathione (μg/mg protein)	3.8±0.7	7.0±0.8	0.05*
GPX (mU/mg protein)	15±4	20±2	0.29
γ-GT (mU/mg protein)	3.3±0.2	2.5±0.9	0.28
Catalase (mKU/mg protein)	46±12	58±5	0.32
SOD (U/mg protein)	143±19	171±20	0.37
Serum vitamin E (μg/ml)	2.9±0.3	2.4±0.2	0.22

Values represent the mean±SE of three lung samples for wild-types (WT) and four lung samples for knockouts (KO). Vitamin E values are obtained from serum, and represent the mean±SE of three serum samples in each group. GPX, glutathione peroxidase activity, γ-GT, gamma glutamyl transferase activity; SOD, total superoxide dismutase activity. *Statistically significant difference between WT and KO.

group means was tested by a single factor ANOVA for multiple groups or unpaired *t* test for two groups (Statview 4.02; Abacus Concepts, Inc., Berkeley, CA). Statistical significance ($P < 0.05$) between and within groups was determined by the Fischer method of multiple comparisons.

Results

Mortality after chronic hyperoxic exposure. To detect a physiologically significant alteration in the knockouts exposed to hyperoxia, a subgroup of animals was exposed to > 95% oxygen continuously until all animals died of oxygen toxicity. Knockouts survived only an average of 8.5±0.5 d, whereas the wild-types survived 13.4±2 d in hyperoxia ($n = 6$ in each group; $P = 0.03$; Fig. 1).

Evaluation of oxidative damage in knockout mice. To detect whether absence of HO-2 was associated with increased lung oxidative stress in sublethal hyperoxic exposure, various parameters of lung oxidative injury were assessed in the animals after 3 d of hyperoxia. In response to hyperoxia, the lungs of HO-2 knockouts had a 1.3-fold higher level of lung protein carbonyls (Fig. 2, *A* and *B*), a 50% lower level of total glutathione, suggesting depletion (Fig. 2 *C*), and higher TBA-RS formation than wild-type animals (0.51±0.02 vs. 0.37±0.02 μmol/mg protein for knockout and wild-type postexposure, respectively; $n = 5$ in each group; $P = 0.005$). Serum LPO were not different between the knockouts and wild-types exposed to hyperoxia. Interestingly, increased lung oxidative injury was also noted in the knockouts before hyperoxic exposure. Lung protein carbonyl content was increased 1.5-fold (Fig. 2, *A* and *B*), serum LPO were increased threefold (8.3±1.6 vs. 2.4±0.9 μmol/liter for knockout and wild-type, respectively; $n = 5$ in each group; $P = 0.02$ vs. wild-type), and formation of lung TBA-RS was significantly higher in the knockout animals compared with the wild-types (0.46±0.04 vs. 0.35±0.01 for

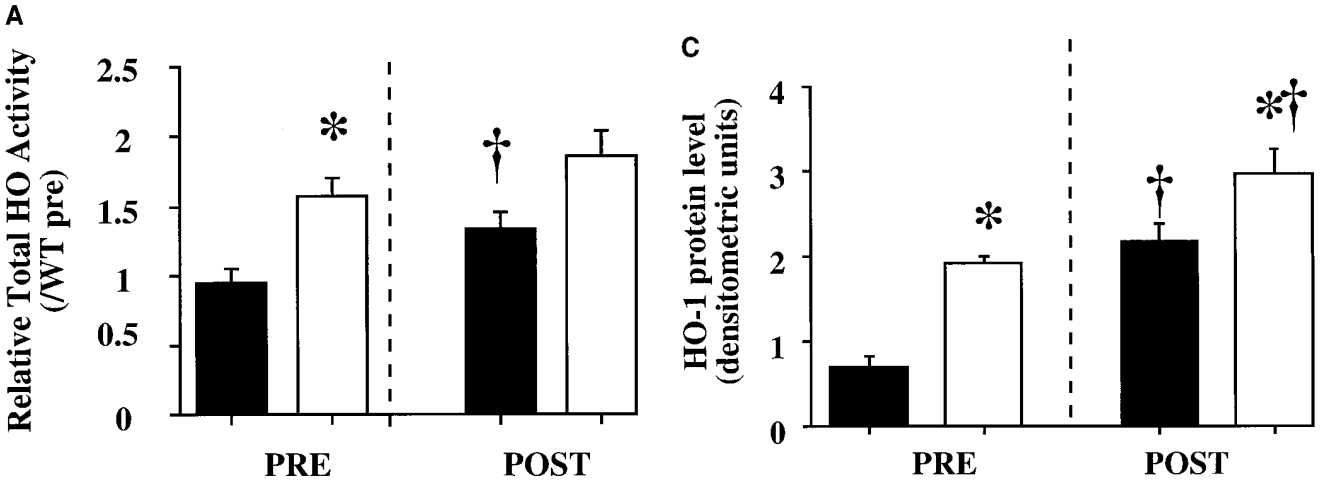

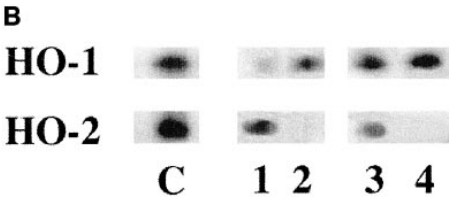

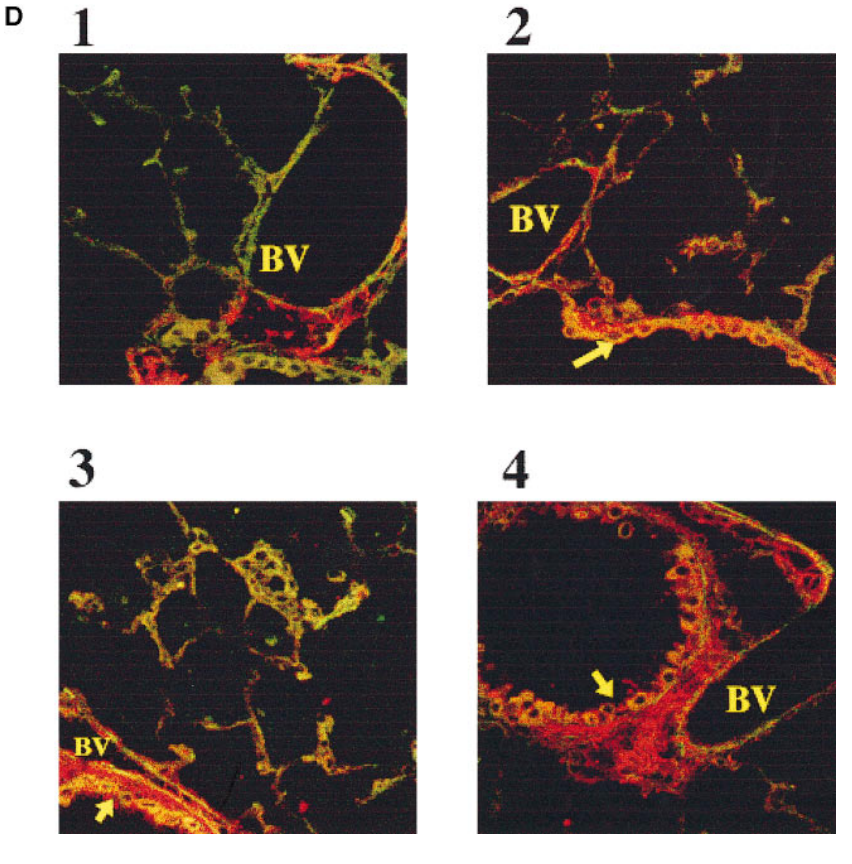

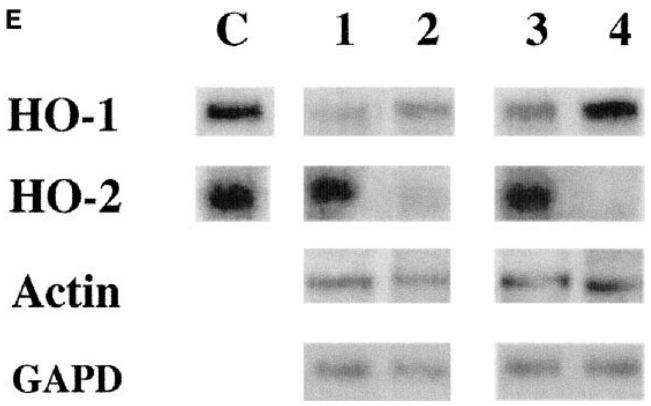

Figure 3. (*A*) Relative total HO activity in the lungs of HO-2 knockout and wild-type mice before and after hyperoxic exposure. Values were derived from the CO content of samples treated with hemin and NADPH (total). Blanks were treated with hemin only, and the (total) minus (blank) value expressed per mg protein of the sample then normalized to the values for the wild-type, preexposure value in each experiment. Each *bar* represents the mean±SE of five lungs from different animals. Knockouts are represented by the *open bars,* and wild-types by the *solid bars.* *$P < 0.05$ vs. wild-type; †$P < 0.05$ vs. same group, preexposure. (*B*) Representative of five Western analyses for HO-immunoreactive protein content in the lungs of HO-2 knockout and wild-type mice before and after hyperoxic exposure. *C*, control derived from cobalt chloride–treated adult rat spleen for HO-1 and untreated adult rat brain for HO-2. Lane *1*, wild-type, preexposure; lane *2*, knockout, preexposure; lane *3*, wild-type, posthyperoxic exposure; lane *4*, knockout, posthyperoxic exposure. (*C*) HO-1 immunoreactive protein content in the lungs of HO-2 knockout and wild-type mice before and after hyperoxic exposure. Samples were subjected to Western analysis, visualized by chemiluminescence, and quantified by densitometry. Densitometric values for each sample were then normalized to the values for the wild-type, preexposure value in each membrane to allow for comparison between membranes. Each *bar* represents the mean±SE of five lung samples from different animals. Knockouts are represented by the *open bars,* and wild-types by the *solid bars.* *$P < 0.05$ vs. wild-type; †$P < 0.05$ vs. same group, preexposure. (*D*) Immunohistochemical localization of HO-1 protein in the lungs of HO-2 knockout and wild-type mice. (*1*) Wild-types, preexposure; (*2*) knockouts, preexposure; (*3*) wild-type,

knockout and wild-type, respectively; $n = 5$ in each group; $P = 0.04$).

Evaluation of basal lung antioxidant levels in knockout mice. Various lung antioxidants and serum vitamin E levels were also determined to ensure that the knockout animals did not have any significant alterations associated with the mutant phenotype that could explain increased susceptibility to hyperoxia. The lungs of HO-2 knockout mice had a significant elevation (twofold increase) in total glutathione content before hyperoxic exposure compared with wild-type animals. None of the other antioxidant enzyme activities or serum vitamin E levels were significantly modified in the transgenic animals compared with wild-type animals (Table I).

Basal heme oxygenase expression in knockout mice. To verify that the lungs of the HO-2 knockout animals had no detectable HO-2, we examined HO expression in these tissues. Surprisingly, HO activity was 1.6-fold higher in the lungs of the HO-2 knockout mice compared with wild-type controls before hyperoxic exposure (Fig. 3 *A*). Upon further examination, lung HO-1 protein levels by Western blotting were elevated twofold in the HO-2 knockouts when compared with controls (Fig. 3, *B* and *C*). As expected, HO-2 protein could not be detected in the lungs of transgenic animals, but was found in the wild-type animals (Fig. 3 *B*). Immunohistochemical detection of HO-1 signal in the lung demonstrated a similar twofold elevation, and revealed that HO-1 did not strictly colocalize with the alveolar macrophages, but was prominently detected in the bronchiolar epithelium and in lung parenchymal cells (Fig. 3 *D*). Endothelial cells also showed moderate expression of HO-1 (Fig. 3 *D*). HO-1 mRNA was barely detectable in the lungs of wild-type animals before hyperoxic exposure, but was found at significantly higher levels (1.5-fold increase) in the lungs of knockout animals (Fig. 3 *E*). In contrast, HO-2 mRNA was not detected in the lungs of transgenic animals, but was expressed in the lungs of wild-type controls (Fig. 3 *E*).

Heme oxygenase expression in knockout mice exposed to hyperoxia. After hyperoxic exposure, total lung HO activity did not significantly change from the preexposure value in the knockout mice (Fig. 3 *A*). However, in the wild-type animals, there was a significant increase in HO activity. Despite this increase, HO activity remained 1.3-fold higher in the lungs of HO-2 knockouts when compared with wild-type controls (Fig. 3 *A*). After 3 d of hyperoxia, lung HO-1 protein levels increased 1.5-fold from the prehyperoxia values in the HO-2 knockout mice, and to a greater extent (2.3-fold increase from preexposure values) in the wild-type animals (Fig. 3, *B* and *C*). In the knockout animals, lung HO-1 protein signal detected by immunohistochemistry was most visibly increased in the peribronchiolar region, and in the endothelial cells after hyperoxic exposure (Fig. 3 *D*). Lung HO-1 mRNA increased 1.5-fold and 2.5-fold, respectively, in the knockout and wild-type animals exposed to hyperoxia (Fig. 3 *E*). HO-2 was undetected in the knockouts, and remained unchanged after hyperoxic exposure in the wild-type mice as verified by densitometry (Fig. 3 *E*).

Evaluation of lung heme, iron, ferritin, and transferrin before and after hyperoxia. To evaluate the contribution of heme to oxidative injury in this model, we measured lung microsomal heme content and evaluated lung hemoprotein content. Lung microsomal heme content of HO-2 knockouts was not significantly different than that of the wild-types both before and after hyperoxic exposure (0.11 ± 0.01 vs. 0.11 ± 0.02 mM/mg protein before exposure, and 0.09 ± 0.01 vs. 0.11 ± 0.01 mM/mg protein after exposure for knockouts and wild-types, respectively). Nonetheless, lung hemoproteins were visibly higher in the knockouts exposed to hyperoxia when compared with similarly exposed wild-type animals (Fig. 4 *A*).

Since HO serves to degrade heme to iron, and this metal is known to be associated with increased oxidative injury (40), we measured total lung iron content and reactive (nonheme) iron. Wild-type and knockout animals had no significant differences in total lung iron content before hyperoxic exposure (Fig. 4 *B*). However, total lung iron increased 3.5-fold in the knockouts after hyperoxic exposure, whereas no significant change in total lung iron was observed in the wild-type animals after hyperoxia (Fig. 4 *B*). This finding was further substantiated by increased iron staining in the lungs of knockout animals exposed to hyperoxia (Fig. 4 *C*). Iron staining in the knockouts was most visible in the endothelial cells and in the peribronchiolar epithelium, a similar distribution as the HO-1 immunoreactive staining demonstrated in Fig. 3 *D*. Reactive (nonheme) iron content was also similar in knockout and wild-type mice before exposure (35.6 ± 2.0 vs. 35.4 ± 2.3 μg/mg protein for knockouts and wild-types, respectively; $n = 5$ in each group). However, this value increased only in the wild-types in response to hyperoxia as measured by the bleomycin assay (42.72 ± 1.4 vs. 58.15 ± 3.9 μg/mg protein for knockouts and wild-types, respectively; $n = 5$ in each group; $P < 0.01$ vs. wild-types).

Iron accumulation could result from increased iron influx through transferrin, or from decreased iron reuse (37). We therefore looked at transferrin receptor levels in the lungs of animals before and after hyperoxia. No differences in transferrin receptor levels could be visualized between knockout and wild-type animals either before or after hyperoxia (Fig. 4 *D*).

Since release of iron is felt to induce ferritin protein, and this may modulate oxidative injury through iron sequestration (41), we evaluated lung ferritin protein by Western analysis and quantitated immunoreactive protein levels by densitome-

Figure 3 legend (Continued)

post–hyperoxic exposure; (*4*) knockouts, post–hyperoxic exposure. Lungs were assayed for immunoreactive protein as described in Methods, and were examined with a Nikon fluorescent microscope at 200×. The red fluorescent signal indicating HO-1 is detectable in both wild-types and knockouts in the cytoplasm of lung parenchymal cells and inflammatory cells and in the peribronchiolar epithelium (*yellow arrows*). However, the signal intensity is visibly higher in the knockouts (*B* and *D*), especially in the peribronchiolar epithelium. After hyperoxic exposure, endothelial cells of lung blood vessels (*BV*) show increased signal intensity in both wild-types and knockouts. The *green signal* representing immunoreactive mature macrophages is partially colocalized to the HO-1 signal in the inflammatory cells. (*E*) Representative of five Northern analyses of HO-1 and HO-2 steady-state levels in the lungs of HO-2 knockout and wild-type mice before and after hyperoxic exposure. *C*, control derived from adult rat spleen after CoCl injection and untreated adult rat brain for HO-2; Lane *1*, wild-type, preexposure; lane *2*, knockout, preexposure; lane 3, wild-type, posthyperoxia; lane *4*, knockout, post hyperoxia. *Lower panels*, β-actin and GAPD signals from the same blot for normalization.

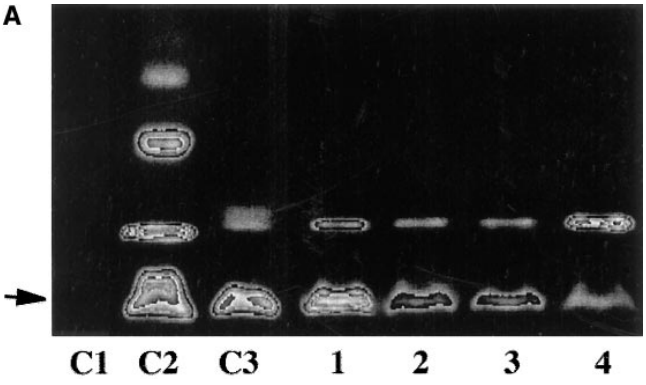

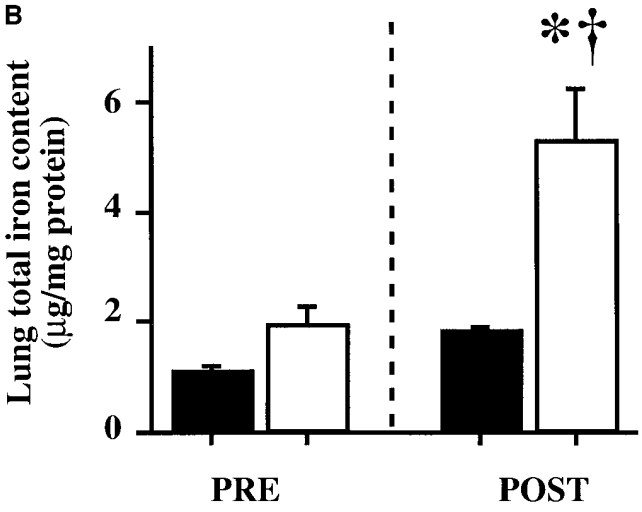

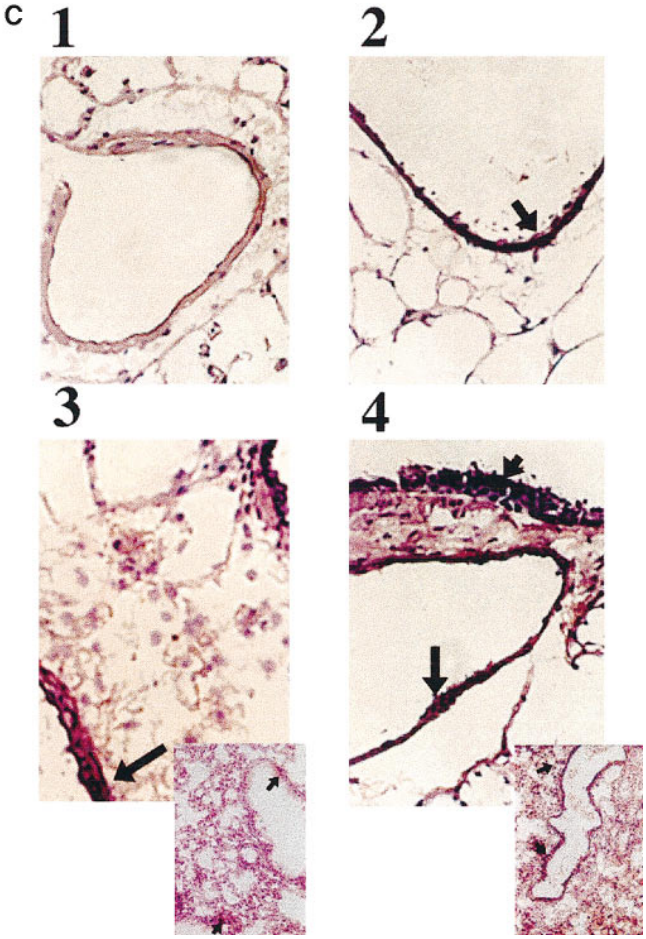

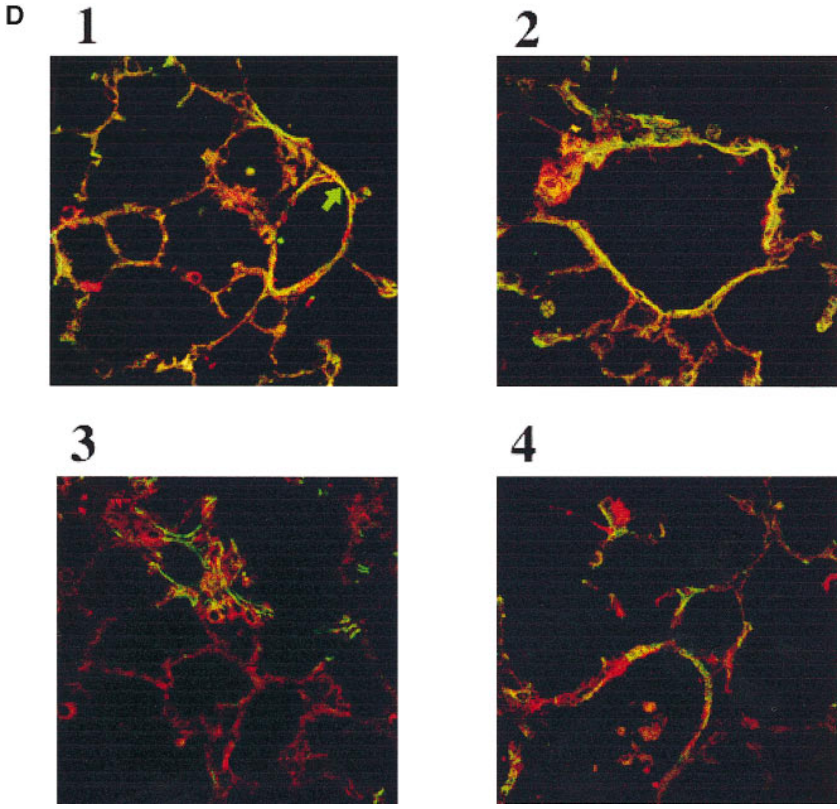

Figure 4. (*A*) Representative of four polyacrylamide gel electrophoreses for detection of lung hemoprotein content of HO-2 knockout and wild-type mice before and after hyperoxic exposure. Lung homogenates (300 μg) were electrophoresed on lithium dodecyl sulfate containing polyacrylamide gels. The gels were then treated with luminol to allow for detection of heme and hemoproteins using a CCD enhanced camera as described in Methods. Lanes *C1–C3*, controls: albumin 100 μg (negative control), cytochrome c (10 μg), and hemoglobin (40 μg), respectively. *Arrow*, migrating free heme front. Lane *1*, wild-type, preexposure; lane *2*, knockout, preexposure; lane *3*, wild-type, posthyperoxic exposure; lane *4*, knockout, posthyperoxic exposure. Other hemoprotein standards (i.e., NO synthase, peroxidase, and catalase) were not shown to migrate in the region of the bands seen in experimental samples, and were therefore excluded. (*B*) Total lung iron content in the lungs of HO-2 knockout and wild-type mice before and after hyperoxic exposure. Values were determined by atomic absorption spectroscopy. Each *bar* represents the mean±SE of four lungs from different animals. Knockouts are represented by the *open bars,* and wild-types by the *solid bars*. $^{*}P < 0.05$ vs. wild-type; $^{\dagger}P < 0.05$ vs. same group, preexposure. (*C*) Iron staining in cryosections of lungs from wild-type and knockout mice before and after exposure to 3 d of hyperoxia. (*1*) Wild-type, preexposure; (*2*) knockouts, preexposure; (*3*) wild-type,

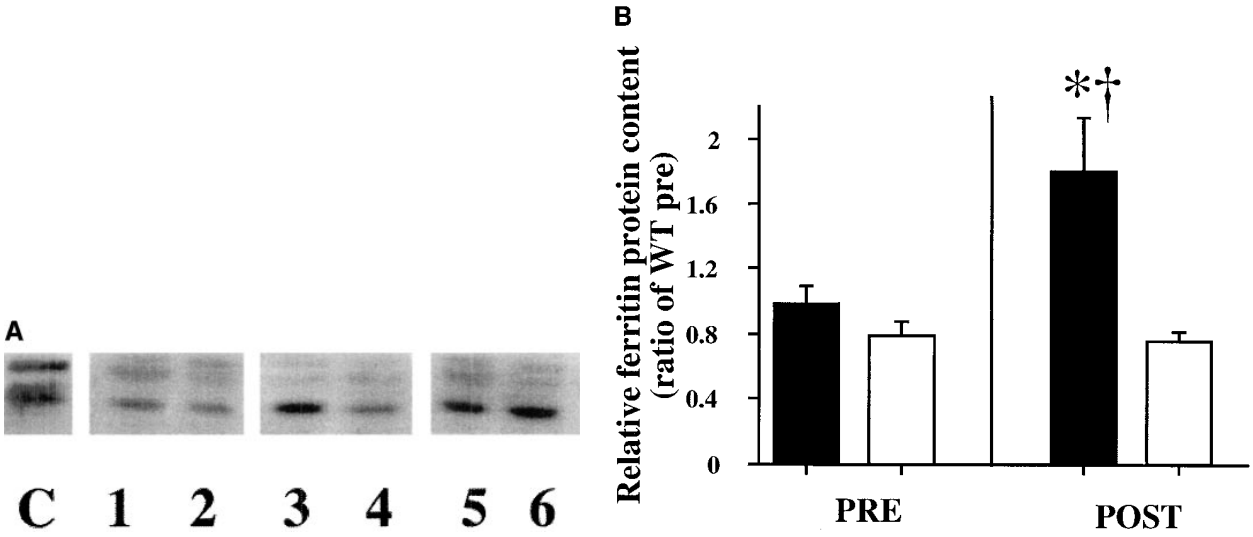

Figure 5. (*A*) Representative of four Western analyses of lung ferritin protein levels in HO-2 knockout and wild-type mice before and after hyperoxic exposure. *C*, control derived from adult rat liver. Lane *1*, wild-type, preexposure; lane *2*, knockout, preexposure; lane *3*, wild-type, posthyperoxic exposure; lane *4*, knockout, posthyperoxic exposure; lane *5*, wild-type injected with hemin; lane *6*, knockout injected with hemin. Equal loading was verified with Coomassie blue staining. (*B*) Relative ferritin protein content of the lungs of HO-2 knockout and wild-type mice before and after hyperoxic exposure. Values were determined by densitometric evaluation of the bands detected in samples represented in *A* (lanes *1–4*). Densitometric values for each sample were then normalized to the values for the wild-type preexposure value in each membrane to allow for comparison between membranes. Each *bar* represents the mean±SE of three lungs from different animals. Knockouts are represented by the *open bars,* and wild-types by the *solid bars*. $^{*}P < 0.05$ vs. wild-type; $^{\dagger}P < 0.05$ vs. same group, preexposure.

try. While ferritin immunoreactive lung protein levels were similar in the knockouts compared with the wild-types before hyperoxic exposure, after hyperoxia the knockouts had a significantly lower level of ferritin protein when compared with the wild-types (Fig. 5, *A* and *B*).

To further understand whether the HO-2 knockouts had an inherent inability to induce ferritin, animals were injected with 15 mg/kg hemin intraperitoneally, and ferritin protein levels were evaluated 24 h later. Knockouts demonstrated increased lung ferritin protein levels after heme injection, as did the wild-types, indicating that there was no abnormality of ferritin production in the knockouts (Fig. 5 *A*).

Since other factors such as nitric oxide (NO) can modulate ferritin expression (38), we evaluated lung protein nitrotyrosine content as an index of NO-mediated damage (39) in the knockout and wild-type animals before and after hyperoxic exposure. Although lung nitrotyrosine content in the wild-types was increased 1.7-fold in hyperoxia compared with preexposure values, the knockouts exposed to hyperoxia had a larger (2.5-fold) increase in lung nitrotyrosine content compared with preexposure values (Fig. 6, *A* and *B*). Therefore, in hyperoxia the knockouts had a 3.2-fold increase in lung nitrotyrosine content when compared with similarly exposed wild-types (Fig. 6, *A* and *B*).

Discussion

It has been speculated that the enzymatic consequences of HO activity may favor increased antioxidant defense by removing a prooxidant heme and forming antioxidant pigments. However, it is not altogether clear why iron released from the heme prosthetic group in the HO reactions would not result in an increased prooxidant burden. Induction of ferritin and consequent sequestering of the released iron may explain restoration of the cellular antioxidant balance in some cases, but this induction response is not universally seen (5, 42). Applegate et al. (10) showed that induction of HO-1 is a generalized response to oxidative stress. Nonetheless, induction of HO-1 in vitro may also serve a specific function, as demonstrated by models of hemin- or hemoglobin-mediated HO-1 induction and HO-1 transfection models (5, 14, 45). Previous studies of the antioxidant role of HO have focused on the inducible HO-1 isoenzyme in cultured cells. We now wanted to determine whether lack of lung HO-2 was associated with diminished re-

Figure 4 legend (Continued)

posthyperoxic exposure; (*4*) knockouts, posthyperoxic exposure. Lung sections were incubated with Perl's solution in the presence of urea-H_2O and DAB and counterstained with Gill no. 3 hematoxylin. The slides were viewed at 400×. Note the more pronounced iron staining (*arrows*) in the parenchymal and endothelial cells of the knockout animals, in particular after hyperoxic exposure. *Insets,* 200× to show general iron distribution. (*D*) Transferrin receptor staining in cryosections of lungs from wild-type and knockout mice before and after exposure to 3 d of hyperoxia. (*1*) Wild-types, preexposure; (*2*) knockouts, preexposure; (*3*) wild-type, posthyperoxic exposure; (*4*) knockouts, posthyperoxic exposure. Lung sections were incubated with FITC-labeled rat anti–mouse transferrin receptor antibodies, and were visualized by confocal microscopy. Immunofluorescent signal (*green arrow*) is most prominent in the lungs of wild-types and knockouts before hyperoxic exposure.

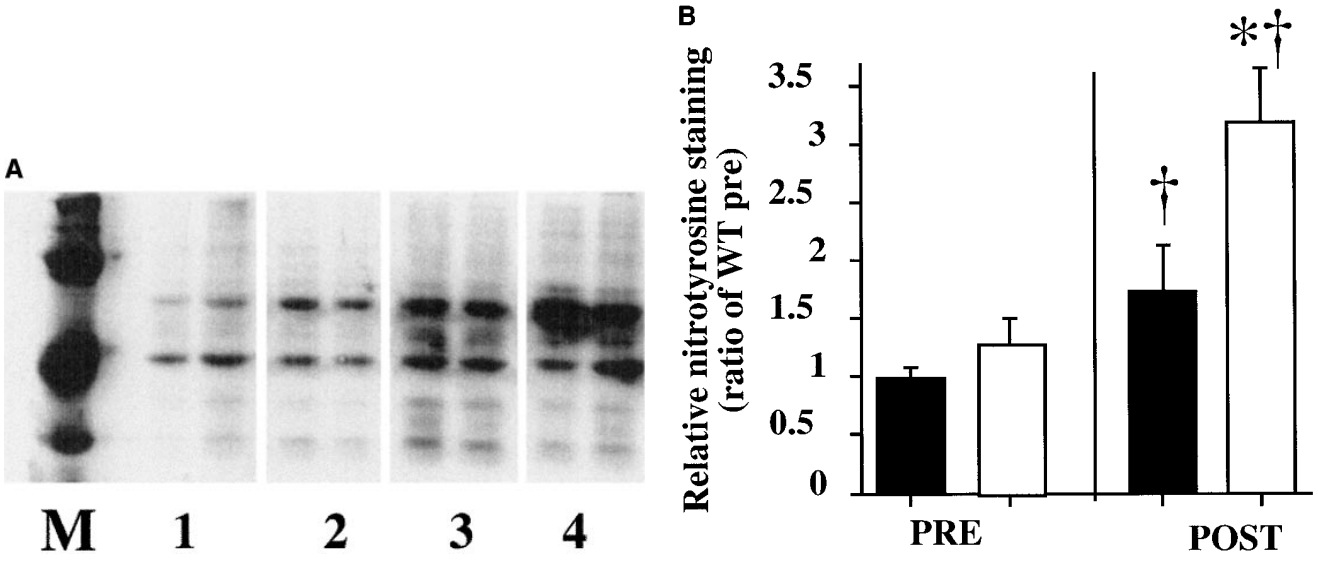

Figure 6. (*A*) Representative of three Western analyses of lung nitrotyrosine content in HO-2 knockout and wild-type mice before and after hyperoxic exposure. *M*, nitrosylated markers. Lane *1*, wild-type, preexposure; lane *2*, knockout, preexposure; lane *3*, wild-type, posthyperoxic exposure; lane *4*, knockout, posthyperoxic exposure. Equal loading was verified with Coomassie blue staining. (*B*) Relative lung nitrotyrosine content in HO-2 knockout and wild-type mice before and after hyperoxic exposure. Values were determined by densitometric evaluation of all bands detected in samples represented in *A*. Densitometric values for each sample were then normalized to the values for the wild-type, preexposure value in each membrane to allow for comparison between membranes. Each *bar* represents the mean±SE of three lungs from different animals. Knockouts are represented by the *open bars*, and wild-types by the *solid bars*. $^{*}P < 0.05$ vs. wild-type; $^{\dagger}P < 0.05$ vs. same group, preexposure.

sistance to lethal and sublethal oxygen toxicity in an in vivo model. The HO-2 knockout mouse demonstrates absence of HO-2 alone, and can help differentiate between HO-1 and HO-2 related effects in vivo.

Knockout animals had substantially increased mortality with chronic hyperoxic exposure, demonstrating a significant physiological alteration in susceptibility to oxygen toxicity. Additionally, the knockouts had increased evidence of lung oxidative injury after a 3-d hyperoxic exposure, as well as before oxygen exposure. The increased susceptibility to oxygen toxicity could not be explained by alterations in other classical antioxidants. In fact, the only difference observed was a significant twofold elevation in lung total glutathione (a potent cellular antioxidant) in the HO-2 knockouts, suggesting that modulation of HO expression results in significant alterations in cellular antioxidant defense leading to compensatory elevation of total glutathione (46). This finding is similar to that observed with HO-1 antisense transfected cells in culture. As with the knockout animals, despite significantly increased total glutathione content compared with controls, these transfected cells were also more susceptible to oxygen toxicity (13).

Increased susceptibility to oxygen toxicity in the HO-2 knockout mice was associated with lack of detectable lung HO-2 protein or HO-2 mRNA as expected, whereas the wild-type animals expressed both isoforms of HO. However, lung total HO activity showed an unanticipated elevation in the knockouts before and after hyperoxic exposure, despite the absence of HO-2. The increased HO activity observed in the lungs of knockout animals seemed to contradict the results of Poss et al. (16), demonstrating lowered total HO activity in tissues of HO-2 knockout animals, particularly in the brain and testes. Logically, eliminating HO-2 would have the most impact on tissues with high HO-2 content, such as the brain and testes. The lung also has a predominance of HO-2, as with the brain and testes, since immunoprecipitation with HO-1 antibodies reduced HO activity to 75% of total (30). Therefore, significantly lowered HO activity was expected in the HO-2 knockouts. However, lung HO-1 protein and HO-1 mRNA were significantly increased in the knockout animals compared with wild-types before and after hyperoxic exposure, suggesting induction of HO-1 due to increased oxidant stress or other mechanisms. Others have demonstrated more ready induction of HO-1 in some cell types such as dermal fibroblasts, with lower HO-2 expression compared with keratinocytes (47). The present results suggest that lung cells are more likely to induce HO-1 than are other tissues.

If HO-1 served to protect against oxidative injury in our in vivo model, it would be expected that normalization of lung HO activity by HO-1 induction would eliminate differences in oxidative stress between the knockouts and wild-types. In view of the increased oxygen toxicity in the HO-2 knockouts despite increased HO-1 expression, it appears that in this model HO-1 induction may be simply a generalized response to oxidative stress, and not necessarily protective. A recent demonstration of a threshold of beneficial effect of HO-1 expression (13) and variable pro- and antioxidant effects of HO-1 in a cell system (43) alludes to the duality of HO-1 as an anti- and prooxidant. Increased oxygen toxicity in the knockouts also suggests that HO-2 provides an essential protective function that may be important in antioxidant defense over and above the effects of HO-1.

To understand further how absence of HO-2 despite increased HO-1 is associated with increased susceptibility to oxidative injury, lung microsomal heme content was evaluated in

wild-type and knockout animals since heme accumulation could result in a prooxidant state (48). Microsomal heme levels were not significantly different between the groups before or after hyperoxia, but this result did not rule out the possibility that the overall heme pools differed. In fact, lung hemoprotein levels were notably increased in the lungs of knockouts as compared with wild-types after hyperoxic exposure, thus likely contributing to enhanced susceptibility to oxidative injury by increasing available redox active iron (49). Additionally, the lungs of knockout animals had a threefold higher total lung iron content than did the wild-types after hyperoxic exposure as detected by atomic absorption spectrometry, suggesting that more redox-active heme or nonheme iron had accumulated in the lungs of the knockouts. Since the knockouts did not have increased non-heme–reactive iron in hyperoxia, whereas the wild-types did, the source of accumulated iron and damaging iron species in the knockouts was likely to be from the lung heme pools, namely the hemoproteins. Furthermore, since lung transferrin receptors were not upregulated in the knockouts exposed to hyperoxia, it is unlikely that the accumulated iron was a result of increased iron transport into the lungs; more likely it was from decreased heme iron turnover. Distribution of the accumulated iron paralleled that of the increased HO-1 signal in the lung after hyperoxia, namely in the endothelial cells and peribronchiolar epithelium, perhaps indicating that HO-1 was induced in areas of increased substrate availability. The possible role of HO-2 in iron turnover somewhat parallels that of HO-1 defined recently in aging HO-1 knockout animals (50). However, in the present model, it is not understood why the altered iron turnover was only unmasked by hyperoxia.

Many authors have documented ferritin coinduction in response to iron release associated with HO-1 induction. This response is felt to be protective (41) since it is well-documented that ferrous iron pools that are not stored in ferritin modulate oxidative injury through generating the hydroxyl radical via the Fenton reaction (51). In this model, no such coinduction of ferritin could be observed in the knockout animals, but was seen in the wild-types. This result is in agreement with the lack of increased lung-reactive iron in the knockouts, and the increased lung-reactive iron in the wild-types, in hyperoxia. Nonetheless, heme-mediated induction of ferritin was readily observed in the knockouts, demonstrating that these animals did not have an inherent inability to produce ferritin. Rather, there may have been a lack of stimulus for ferritin induction since no increase in reactive (nonheme) iron was observed. However, the lack of increased lung-reactive iron in the knockouts does not explain why the accumulated heme iron seen would have not resulted in ferritin induction.

Ferritin synthesis is modulated by the iron response element binding protein (IRE-BP). NO is a molecule that can decrease ferritin expression by activating the iron response element though IRE-BP, which in turn represses ferritin mRNA translation (38). Evidence of increased NO was demonstrated by increased nitrotyrosine residues in the lungs of knockout animals after hyperoxia. Increased NO production in hyperoxia has previously been observed (39, 53), but it is not clear why absence of HO-2 was associated with even higher NO production in the knockouts. Another possibility to explain why lung ferritin was not induced in the knockouts is decreased ferritin synthesis resulting from severe oxidative stress, as shown in another model (54). In any case, lowered lung ferritin content in the knockout animals may have further predisposed the animals to lung oxidative injury.

Recent work suggests that HO-2 may serve to bind heme since it has two heme-binding sites independent of the heme catalytic site (15). Therefore, absence of HO-2 could result in increased heme available for oxidative reactions. In this model, we conclude that absence of HO-2 results in increased hyperoxic injury in vivo due to accumulation of heme-derived iron. This heme accumulation also appears to lead to enhanced HO-1 induction, which in the absence of ferritin coinduction may result in increased availability of redox active iron. We therefore propose that HO-2 is important in iron turnover during oxidative stress. Finally, we caution that therapeutic strategies that may inhibit HO-2 could result in enhanced oxidative injury and iron accumulation.

Acknowledgments

We thank Kunju J. Sridhar, Ph.D., Monika Bhatia, and Julia E. Sim for their expert technical assistance. We are indebted to Philip Huie, Ph.D., for his invaluable expertise in histochemical techniques, and to Christopher Contag, Ph.D., for expertise in the use of the CCD enhancer camera. We gratefully acknowledge the assistance of Pamela Contag, Ph.D., and Denise Suttner, M.D., in the preparation and amplification of the HO-2 cDNA probe. We also acknowledge the contribution of Dr. Susumu Tonegawa in the development and maintenance of the mutant strains.

This work was funded by the National Institutes of Health grants HL-52701 (P.A. Dennery) and HL-51469 (D.R. Spitz), and the Mary L. Johnson and Hess funds of Stanford University.

References

1. Keyse, S.M., L.A. Applegate, Y. Tromvoukis, and R.M. Tyrrell. 1990. Oxidant stress leads to transcriptional activation of the human heme oxygenase gene in cultured skin fibroblasts. *Mol. Cell. Biol.* 10:4967–4969.

2. Vile, G.F., S. Basu-Modak, C. Waltner, and R.M. Tyrrell. 1994. Heme oxygenase 1 mediates an adaptive response to oxidative stress in human skin fibroblasts. *Proc. Natl. Acad. Sci. USA*. 91:2607–2610.

3. Lautier, D., P. Luscher, and R.M. Tyrrell. 1992. Endogenous glutathione levels modulate both constitutive and UVA radiation/hydrogen peroxide inducible expression of the human heme oxygenase gene. *Carcinogenesis*. 13:227–232.

4. Choi, A.M., K. Knobil, S.L. Otterbein, D.A. Eastman, and D.B. Jacoby. 1996. Oxidant stress responses in influenza virus pneumonia: gene expression and transcription factor activation. *Am. J. Physiol.* 271:L383–L391.

5. Dennery, P.A., H.E. Wong, K.J. Sridhar, P.A. Rodgers, J.E. Sim, and D.R. Spitz. 1996. Differences in basal and hyperoxia-associated HO expression in oxidant-resistant hamster fibroblasts. *Am. J. Physiol.* 271:L672–L679.

6. Lee, P.J., J. Alam, S.L. Sylvester, N. Inamdar, L. Otterbein, and A.M. Choi. 1996. Regulation of heme oxygenase-1 expression in vivo and in vitro in hyperoxic lung injury. *Am. J. Respir. Cell Mol. Biol*. 14:556–568.

7. Jornot, L., and A.F. Junod. 1993. Variable glutathione levels and expression of antioxidant enzymes in human endothelial cells. *Am. J. Physiol*. 264: L482–L489.

8. Saunders, E.L., M.D. Maines, M.J. Meredith, and M.L. Freeman. 1991. Enhancement of heme oxygenase-1 synthesis by glutathione depletion in Chinese hamster ovary cells. *Arch. Biochem. Biophys*. 288:368–373.

9. Ewing, J.F., and M.D. Maines. 1993. Glutathione depletion induces heme oxygenase-1 (HSP32) mRNA and protein in rat brain. *J. Neurochem*. 60:1512–1519.

10. Applegate, L.A., P. Luscher, and R.M. Tyrrell. 1991. Induction of heme oxygenase: a general response to oxidant stress in cultured mammalian cells. *Cancer Res*. 51:974–978.

11. Alam, J., and Z. Den. 1992. Distal AP-1 binding sites mediate basal level enhancement and TPA induction of the mouse heme oxygenase-1 gene. *J. Biol. Chem*. 267:21894–21900.

12. Eisenstein, R.S., M.D. Garcia, W. Pettingell, and H.N. Munro. 1991. Regulation of ferritin and heme oxygenase synthesis in rat fibroblasts by different forms of iron. *Proc. Natl. Acad. Sci. USA*. 88:688–692.

13. Dennery, P., K. Sridhar, C. Lee, H. Wong, V. Shokoohi, P. Rodgers, and D. Spitz. 1997. Heme oxygenase-mediated resistance to oxygen toxicity in hamster fibroblasts. *J. Biol. Chem*. 272:14937–14942.

14. Lee, P.J., J. Alam, G.W. Wiegand, and A.M. Choi. 1996. Overexpression of heme oxygenase-1 in human pulmonary epithelial cells results in cell growth arrest and increased resistance to hyperoxia. *Proc. Natl. Acad. Sci. USA*. 93:10393–10398.

15. McCoubrey, W.K., Jr., T.J. Huang, and M.D. Maines. 1997. Heme oxygenase-2 is a hemoprotein and binds heme through heme regulatory motifs that are not involved in heme catalysis. *J. Biol. Chem*. 272:12568–12574.

16. Poss, K.D., M.J. Thomas, A.K. Ebralidze, T.J. O'Dell, and S. Tonegawa. 1995. Hippocampal long-term potentiation is normal in heme oxygenase-2 mutant mice. *Neuron*. 15:867–873.

17. Wright, J.R., H.D. Colby, and P.R. Miles. 1981. Cytosolic factors which affect microsomal lipid peroxidation in lung and liver. *Arch. Biochem. Biophys*. 206:296–304.

18. Schacter, E., J.A. Williams, M. Lim, and R.L. Levine. 1994. Differential susceptibility of plasma proteins to oxidative modification: examination by western blot immunoassay. *Free Radical Biol. Med*. 17:429–437.

19. Lowry, O., H. Rosebrough, A. Farr, and R. Randall. 1951. Protein measurement with the Folin phenol reagent. *J. Biol. Chem*. 193:265–272.

20. Anderson, M.E. 1985. Determination of glutathione and glutathione disulfide in biological samples. *Methods Enzymol*. 113:548–555.

21. Lawrence, R.A., and R.F. Burk. 1976. Glutathione peroxidase activity in selenium-deficient rat liver. *Biochem. Biophys. Res. Commun*. 71:952–958.

22. Beers, R.F., and I.W. Sizer. 1952. A spectrophotometric method for measuring the breakdown of H2O2 by catalase. *J. Biol. Chem.* 195:133–140.

23. Aebi, H. 1984. Catalase in vitro. *Methods Enzymol*. 105:121–126.

24. Spitz, D.R., and L.W. Oberley. 1989. An assay for superoxide dismutase activity in mammalian tissue homogenates. *Anal. Biochem*. 179:8–18.

25. Vreman, H.J., and D.K. Stevenson. 1988. Heme oxygenase activity as measured by carbon monoxide production. *Anal. Biochem*. 168:31–38.

26. Wilks, A., and P.R. Ortiz de Montellano. 1993. Rat liver heme oxygenase. High level expression of a truncated soluble form and nature of the meso-hydroxylating species. *J. Biol. Chem*. 268:22357–22362.

27. Sambrook, J., E. Fritsch, and T. Maniatis. Molecular Cloning: A Laboratory Manual. 1989. Cold Spring Harbor Laboratory, Cold Spring Harbor, NY.

28. Feinberg, A.P., and B. Vogelstein. 1983. A technique for radiolabeling DNA restriction endonuclease fragments to high specific activity. *Anal. Biochem*. 132:6–13.

29. Chomczynski, P., and N. Sacchi. 1987. Single-step method of RNA isolation by acid guanidinium thiocyanate-phenol-chloroform extraction. *Anal. Biochem*. 162:156–159.

30. Dennery, P.A., P.A. Rodgers, M.A. Lum, B.C. Jennings, and V. Shokoohi. 1996. Hyperoxic regulation of lung heme oxygenase in neonatal rats. *Pediatr. Res*. 40:815–821.

31. Smith, M.L., and W.S. Caughey. 1978. New methods for isolation and characterization of hemes. *Methods Enzymol*. 52:421–436.

32. Bonfils, C., S. Charasse, J.P. Bonfils, and C. Larroque. 1995. Luminescent visualization of low amounts of cytochrome P450 and hemoproteins by luminol in acrylamide gels. *Anal. Biochem*. 226:302–306.

33. van Deursen, C.T., M.P. van Dieijen-Visser, J. Koudstaal, and P.J. Brombacher. 1989. Determination of tissue iron and ferritin in liver pathology comparison of histochemical and biochemical results. *J. Clin. Chem. Clin. Biochem*. 27:345–349.

34. Evans, P.J., and B. Halliwell. 1994. Measurement of iron and copper in biological systems: bleomycin and copper-phenanthroline assays. *Methods Enzymol*. 233:82–92.

35. Gutteridge, J.M., D.A. Rowley, and B. Halliwell. 1981. Superoxide-dependent formation of hydroxyl radicals in the presence of iron salts. Detection of 'free' iron in biological systems by using bleomycin-dependent degradation of DNA. *Biochem. J*. 199:263–265.

36. Hill, J.M., and R.C. Switzer III. 1984. The regional distribution and cellular localization of iron in the rat brain. *Neuroscience*. 11:595–603.

37. Kuhn, L.C. 1994. Molecular regulation of iron proteins. *Bailliere's Clin. Haematol*. 7:763–785.

38. Pantopoulos, K., and M.W. Hentze. 1995. Nitric oxide signaling to iron-regulatory protein: direct control of ferritin mRNA translation and transferrin receptor mRNA stability in transfected fibroblasts. *Proc. Natl. Acad. Sci. USA*. 92:1267–1271.

39. Haddad, I.Y., G. Pataki, P. Hu, C. Galliani, J.S. Beckman, and S. Matalon. 1994. Quantitation of nitrotyrosine levels in lung sections of patients and animals with acute lung injury. *J. Clin. Invest*. 94:2407–2413.

40. Ryan, T.P., and S.D. Aust. 1992. The role of iron in oxygen-mediated toxicities. *Crit. Rev. Toxicol*. 22:119–141.

41. Balla, G., H.S. Jacob, J. Balla, M. Rosenberg, K. Nath, F. Apple, J.W. Eaton, and G.M. Vercellotti. 1992. Ferritin: a cytoprotective antioxidant strategem of endothelium. *J. Biol. Chem*. 267:18148–18153.

42. Tom, D.J., P.A. Rodgers, V. Shokoohi, D.K. Stevenson, and P.A. Dennery. 1996. Hepatic heme oxygenase is inducible in neonatal rats during the early postnatal period. *Pediatr. Res*. 40:288–293.

43. da Silva, J.L., T. Morishita, B. Escalante, R. Staudinger, G. Drummond, M.S. Goligorsky, J.D. Lutton, and N.G. Abraham. 1996. Dual role of heme oxygenase in epithelial cell injury: contrasting effects of short-term and long-term exposure to oxidant stress. *J. Lab. Clin. Med*. 128:290–296.

44. Otterbein, L., S.L. Sylvester, and A.M. Choi. 1995. Hemoglobin provides protection against lethal endotoxemia in rats: the role of heme oxygenase-1. *Am. J. Respir. Cell Mol. Biol*. 13:595–601.

45. Abraham, N.G., Y. Lavrovsky, M.L. Schwartzman, R.A. Stoltz, R.D. Levere, M.E. Gerritsen, S. Shibahara, and A. Kappas. 1995. Transfection of the human heme oxygenase gene into rabbit coronary microvessel endothelial cells: protective effect against heme and hemoglobin toxicity. *Proc. Natl. Acad. Sci. USA*. 92:6798–6802.

46. Knickelbein, R.G., D.H. Ingbar, T. Seres, K. Snow, R.B. Johnston, Jr., O. Fayemi, F. Gumkowski, J.D. Jamieson, and J.B. Warshaw. 1996. Hyperoxia enhances expression of gamma-glutamyl transpeptidase and increases protein S-glutathiolation in rat lung. *Am. J. Physiol*. 270:L115–L122.

47. Applegate, L.A., A. Noel, G. Vile, E. Frenk, and R.M. Tyrrell. 1995. Two genes contribute to different extents to the heme oxygenase enzyme activity measured in cultured human skin fibroblasts and keratinocytes: implications for protection against oxidant stress. *Photochem. Photobiol*. 61:285–291.

48. Vercellotti, G.M., G. Balla, J. Balla, K. Nath, J.W. Eaton, and H.S. Jacob. 1994. Heme and the vasculature: an oxidative hazard that induces antioxidant defenses in the endothelium. *Artif. Cells Blood Substit. Immobil. Biotechnol*. 22:207–213.

49. Giulivi, C., and E. Cadenas. 1993. The reaction of ascorbic acid with different heme iron redox states of myoglobin. Antioxidant and prooxidant aspects. *FEBS Lett*. 332:287–290.

50. Poss, K.D., and S. Tonegawa. 1997. Heme oxygenase 1 is required for mammalian iron reutilization. *Proc. Natl. Acad. Sci. USA*. 94:10919–10924.

51. Rothman, R.J., A. Serroni, and J.L. Farber. 1992. Cellular pool of transient ferric iron, chelatable by deferoxamine and distinct from ferritin, that is involved in oxidative cell injury. *Mol. Pharmacol*. 42:703–710.

52. Haile, D.J., T.A. Rouault, C.K. Tang, J. Chin, J.B. Harford, and R.D. Klausner. 1992. Reciprocal control of RNA-binding and aconitase activity in the regulation of the iron-responsive element binding protein: role of the iron-sulfur cluster. *Proc. Natl. Acad. Sci. USA*. 89:7536–7540.

53. Garat, C., C. Jayr, S. Eddahibi, M. Laffon, M. Meignan, and S. Adnot. 1997. Effects of inhaled nitric oxide or inhibition of endogenous nitric oxide formation on hyperoxic lung injury. *Am. J. Respir. Crit. Care Med*. 155:1957–1964.

54. Pantopoulos, K., and M.W. Hentze. 1995. Rapid responses to oxidative stress mediated by iron regulatory protein. *EMBO (Eur. Mol. Biol. Organ.) J*. 14:2917–2924.